

## Piezoelectric energy harvesting with parametric uncertainty

This article has been downloaded from IOPscience. Please scroll down to see the full text article.

2010 Smart Mater. Struct. 19 105010

(<http://iopscience.iop.org/0964-1726/19/10/105010>)

View [the table of contents for this issue](#), or go to the [journal homepage](#) for more

Download details:

IP Address: 137.222.10.113

The article was downloaded on 07/08/2010 at 12:00

Please note that [terms and conditions apply](#).

# Piezoelectric energy harvesting with parametric uncertainty

S F Ali, M I Friswell and S Adhikari

School of Engineering, Swansea University, Singleton Park, Swansea SA2 8PP, UK

E-mail: [sk.faruque.ali@gmail.com](mailto:sk.faruque.ali@gmail.com), [M.I.Friswell@swansea.ac.uk](mailto:M.I.Friswell@swansea.ac.uk) and [S.Adhikari@swansea.ac.uk](mailto:S.Adhikari@swansea.ac.uk)

Received 15 April 2010, in final form 16 July 2010

Published 6 August 2010

Online at [stacks.iop.org/SMS/19/105010](http://stacks.iop.org/SMS/19/105010)

## Abstract

The design and analysis of energy harvesting devices is becoming increasingly important in recent years. Most of the literature has focused on the deterministic analysis of these systems and the problem of uncertain parameters has received less attention. Energy harvesting devices exhibit parametric uncertainty due to errors in measurement, errors in modelling and variability in the parameters during manufacture. This paper investigates the effect of parametric uncertainty in the mechanical system on the harvested power, and derives approximate explicit formulae for the optimal electrical parameters that maximize the mean harvested power. The maximum of the mean harvested power decreases with increasing uncertainty, and the optimal frequency at which the maximum mean power occurs shifts. The effect of the parameter variance on the optimal electrical time constant and optimal coupling coefficient are reported. Monte Carlo based simulation results are used to further analyse the system under parametric uncertainty.

(Some figures in this article are in colour only in the electronic version)

## 1. Introduction

Recent developments in automation, wireless technology and smart systems have necessitated the development of self- and low-powered sensors and actuators. Many of these sensors convert ambient energy sources such as thermal, mechanical, chemical, optical or biochemical into electrical energy. The objective of energy harvesting is to collect ambient energy and power electronic systems. Various concepts to harvest energy from ambient vibration of the host system have been proposed [1–6]. Reviews on energy harvesting from mechanical and biological systems are given by references [1, 5, 6]. A comparison of four different vibration-powered generators designed for standalone systems is reported in [3, 4].

Energy harvesting of ambient vibration has become important as new electronic devices are being developed that require very low power and a complete ‘self-power’ system gives a long service life. Harvesting is attractive because harvested energy can be used directly or used to recharge batteries or other storage devices, which enhances battery life and reduces maintenance cost. Applications include wireless sensor systems that are desirable in biological implants,

robotic devices and structural health monitoring, where remote operations are required. This can only be accomplished by using chargeable batteries that store harvested energy and/or by directly using the harvested energy. Furthermore, energy harvesting reduces regular monitoring costs.

Many vibration energy harvesters explore the ability of active materials, such as piezoelectric materials, to generate electric charge in response to external mechanical vibrations [7–10]. Of the published results that focus on the piezoelectric effect as the transduction method, almost all have focused on harvesting using cantilever beams and on single frequency ambient energy, i.e., resonance based energy harvesting. The exceptions are Sodano *et al* [7] who investigated random ambient vibration disturbances and Tanner *et al* [8] who developed a piezoceramic stack harvesting device to power a magneto-rheological damper.

Soliman *et al* [11] considered energy harvesting under wide band excitation. Wide band harvesters are reported to scavenge more power compared to single frequency harvesters, as shown by Soliman *et al* [11] who replaced a linear oscillator with a piecewise linear oscillator as the energy harvesting element. Liu *et al* [12] proposed acoustic energy harvesting using an electromechanical resonator. Shu *et al*

[13–15] conducted detailed analysis of the power output for piezoelectric energy harvesting systems. The relationship between the energy conversion efficiency, electrically induced damping and power transfer for a rectified piezoelectric power harvester was developed in [13]. Shu *et al* [14] investigated the parameters for optimal power generation in a rectified piezoelectric device. The results showed that the harvested power depends on the input vibration characteristics (frequency and acceleration), the mass of the generator, the electrical load, the natural frequency, the mechanical damping ratio and the electromechanical coupling coefficient of the system. The conclusions were validated experimentally. Several other authors [16–19] have also proposed methods to optimize the parameters of the system to maximize the harvested energy.

The design of an energy harvesting device must be tailored to the ambient energy available [14]. In some applications the ambient excitation will be at a single frequency, and most studies have designed resonant harvesting devices based on this. Such devices have to be tuned to the excitation and may not be robust to variations in the excitation frequency. Adhikari *et al* [9, 10] developed a probabilistic framework for piezoelectric energy harvesters, where the input excitation was random, although they assumed that the system parameters were deterministic, i.e. the parameters were known exactly. The effect of parametric uncertainty on the harvested energy has received little attention. Determining exact single natural frequency and damping characteristics of a real distributed system that is modelled as a single degree of freedom (SDOF) system can lead to errors. If the system exists then the modal properties may be measured, although errors due to noise and the estimation method will always be present. Furthermore there is variability in the devices due to the manufacturing variability, or variability in operation due to changes in the environment. Slight perturbations in the natural frequency of the mechanical system can lead to an alarming decrease in the harvested electrical power, and is the subject of this paper.

Most studies [1–6] assume the mechanical parameters are deterministic and that the excitation is harmonic. A few studies [9, 11] considered broadband random excitation. The effect on the harvested power when the mechanical system parameters are uncertain appears to have received little attention in the literature. The theory is developed in this paper for the case when the parameters of the mechanical system are random. The parametric uncertainties in this paper are considered to be uncorrelated and their joint effects on harvested power are not analysed. To the authors' knowledge, the nature and level of correlation between various uncertain parameters are not available in the literature. However, in the context of structural dynamics and vibroacoustics, some authors have attempted to quantify uncertainty in the system parameters using experimental approaches. For example, Kompella and Bernhard [20] measured 57 frequency response functions at driver microphones for different pickup trucks. Fahy [21] reported measurements of FRFs on 41 nominally identical beer cans. More recently, Adhikari *et al* [22] considered uncertainty in the mass distribution in beams and plates. In their work 2% uncertainty in the mass distribution

in a beam and 10% uncertainty in the stiffness of attached oscillators in a plate were considered. The majority of these experiential works, as well as the theoretical works (e.g., [23]), assume an uncertainty model (e.g., Gaussian) and then select some values of the mean and standard deviation of the parameter of interest. The deterministic analysis can be viewed as a special case when the standard deviation is zero. In this paper we consider up to 20% uncertainty in the parameters. While there may be situations where uncertainties may be more, the results give an indication as to what one might expect within this range of uncertainty. For example it will be shown later in section 4 that the harvested power decreases abruptly with the increase in standard deviation of natural frequency of the system. Therefore it is expected that change in harvested power could change the optimal electrical parameters. This study develops a semi-analytical approach to determine the effect of uncertainty on the optimal electrical parameters. Numerical results obtained using Monte Carlo Simulation are also reported.

The outline of the paper is as follows. A SDOF electromechanical model under deterministic excitation with random parameters is discussed in section 2. The mean power for a piezoelectric system is derived in section 3. The effect on the harvested power due to changes to the uncertainty in the mechanical parameters of the system is discussed in section 4. Optimal electrical parameters due to random mechanical parameters are derived in section 5 and approximate formulae are given as functions of the standard deviation of the random parameters. Numerical studies using Monte Carlo simulations (MCS) are reported in section 6. Based on the study undertaken in the paper, a set of conclusions are drawn in section 7.

## 2. Single degree of freedom deterministic electromechanical model

We consider a stack type piezoelectric harvesting circuit without an inductor as shown in figure 1. Energy is harvested through base excitations and the piezoceramic is operated in the {33} direction. Here we use a simple SDOF model for the mechanical motion of the harvester. Erturk and Inman [24–27] gave a more detailed model, along with correction factors for an SDOF model that accounts for distributed mass effects. This enables the analysis described here to be used in a wide range of practical applications. The SDOF model could be extended to multidegree of freedom mechanical systems by using a modal decomposition of the response. This paper only considers a linear model of the piezoelectric material along the d33 direction, which allows the application of linear vibration theory.

duToit and Wardle [28] expressed the coupled electromechanical behaviour by the coupled linear ordinary differential equations

$$m\ddot{x}(t) + c\dot{x}(t) + kx(t) - \theta v(t) = -m\ddot{x}_b(t) \quad (1)$$

$$\theta\dot{x}(t) + C_p\dot{v}(t) + \frac{1}{R_l}v(t) = 0. \quad (2)$$

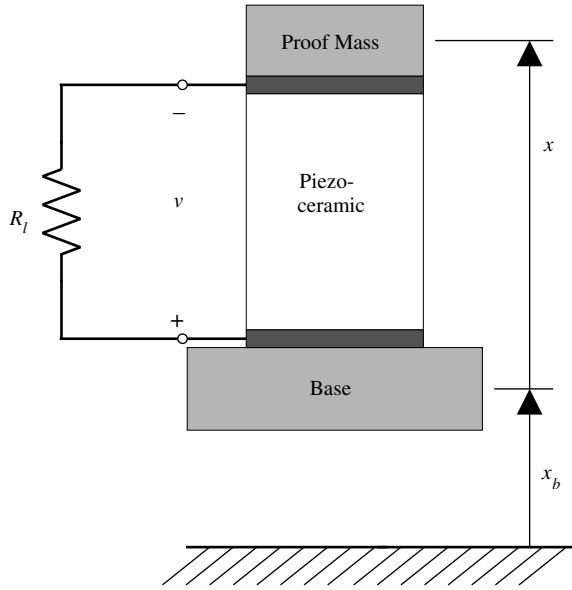


**Figure 1.** Schematic diagrams of piezoelectric energy harvesters without inductor.

Equation (1) is simply Newton's equation of motion for a SDOF system, where  $t$  is the time,  $x(t)$  is the displacement of the mass,  $m$ ,  $c$  and  $k$  are respectively the mass, damping and stiffness of the harvester and  $x_b(t)$  is the base excitation.  $\theta$  is the electromechanical coupling, and the mechanical force is modelled as proportional to the voltage across the piezoceramic,  $v(t)$ . Equation (2) is obtained from the electrical circuit, where the voltage across the load resistance arises from the mechanical strain through the electromechanical coupling,  $\theta$ , and the capacitance of the piezoceramic,  $C_p$ . We assume the mass to be known perfectly but there is uncertainty in the estimation of the stiffness and damping of the harvester. Therefore, we consider the natural frequency and the damping coefficient to be random processes. The coupling coefficient may also be uncertain, and this is considered further in section 4.

Transforming equations (1) and (2) into the frequency domain and dividing the first equation by  $m$  and the second equation by  $C_p$ , we obtain

$$(-\omega^2 + 2i\omega\zeta\omega_n + \omega_n^2)X(\omega) - \frac{\theta}{m}V(\omega) = \omega^2 X_b(\omega) \quad (3)$$

$$i\omega \frac{\theta}{C_p} X(\omega) + \left( i\omega + \frac{1}{C_p R_l} \right) V(\omega) = 0 \quad (4)$$

where  $X(\omega)$ ,  $V(\omega)$  and  $X_b(\omega)$  are the Fourier transforms of  $x(t)$ ,  $v(t)$  and  $x_b(t)$ , respectively. The natural frequency of the harvester,  $\omega_n$ , and the damping factor,  $\zeta$ , are assumed to be random in nature and are defined as

$$\omega_n = \bar{\omega}_n \Psi_\omega \quad (5)$$

$$\zeta = \bar{\zeta} \Psi_\zeta \quad (6)$$

where  $\Psi_\omega$  and  $\Psi_\zeta$  are the multiplicative random parts of the natural frequency and damping coefficient.  $\bar{\omega}_n$  and  $\bar{\zeta}$  are the

mean values of the natural frequency and damping coefficient, given by

$$\bar{\omega}_n = \sqrt{\frac{\bar{k}}{m}} \quad \text{and} \quad \bar{\zeta} = \frac{\bar{c}}{2m\bar{\omega}_n}. \quad (7)$$

where  $\bar{k}$  and  $\bar{c}$  are the mean value of the stiffness and damping of the system respectively. Combining equations (3)–(6), we get

$$(-\omega^2 + 2i\omega\bar{\zeta}\bar{\omega}_n\Psi_\omega\Psi_\zeta + \bar{\omega}_n^2\Psi_\omega^2)X(\omega) - \frac{\theta}{m}V(\omega) = \omega^2 X_b(\omega) \quad (8)$$

$$i\omega \frac{\theta}{C_p} X(\omega) + \left( i\omega + \frac{1}{C_p R_l} \right) V(\omega) = 0. \quad (9)$$

Dividing equation (8) by  $\bar{\omega}_n^2$  and equation (9) by  $\bar{\omega}_n$  and writing in a matrix form one has

$$\begin{bmatrix} (\Psi_\omega^2 - \Omega^2 + 2i\Omega\bar{\zeta}\Psi_\omega\Psi_\zeta) & -\frac{\theta}{\bar{k}} \\ i\Omega\frac{\alpha\theta}{C_p} & (i\Omega\alpha + 1) \end{bmatrix} \begin{Bmatrix} X \\ V \end{Bmatrix} = \begin{Bmatrix} \Omega^2 X_b \\ 0 \end{Bmatrix}, \quad (10)$$

where the dimensionless frequency and dimensionless time constant are defined as

$$\Omega = \frac{\omega}{\bar{\omega}_n} \quad \text{and} \quad \alpha = \bar{\omega}_n C_p R_l. \quad (11)$$

Here  $\alpha$  is the time constant of the first order electrical system, non-dimensionalized using the natural frequency of the mechanical system. Inverting the coefficient matrix, the displacement and voltage in the frequency domain can be obtained as

$$\begin{Bmatrix} X \\ V \end{Bmatrix} = \frac{1}{\Delta_1} \begin{bmatrix} (i\Omega\alpha + 1) & \frac{\theta}{\bar{k}} \\ -i\Omega\frac{\alpha\theta}{C_p} & (\Psi_\omega^2 - \Omega^2 + 2i\Omega\bar{\zeta}\Psi_\omega\Psi_\zeta) \end{bmatrix} \times \begin{Bmatrix} \Omega^2 X_b \\ 0 \end{Bmatrix} = \begin{Bmatrix} (i\Omega\alpha + 1)\Omega^2 X_b / \Delta_1 \\ -i\Omega^3 \frac{\alpha\theta}{C_p} X_b / \Delta_1 \end{Bmatrix} \quad (12)$$

where the determinant of the coefficient matrix is

$$\Delta_1(i\Omega, \Psi_\omega, \Psi_\zeta) = (i\Omega)^3 \alpha + (2\bar{\zeta}\alpha\Psi_\omega\Psi_\zeta + 1)(i\Omega)^2 + (\alpha\Psi_\omega^2 + \kappa^2\alpha + 2\bar{\zeta}\Psi_\omega\Psi_\zeta)(i\Omega) + \Psi_\omega^2 \quad (13)$$

and the non-dimensional electromechanical coupling coefficient is

$$\kappa^2 = \frac{\theta^2}{\bar{k}C_p}. \quad (14)$$

### 3. Mean harvested power from harmonic excitation

From equation (12) we obtain the voltage in the frequency domain as

$$V = \frac{-i\Omega^3 \frac{\alpha\theta}{C_p}}{\Delta_1(i\Omega, \Psi_\omega, \Psi_\zeta)} X_b. \quad (15)$$

Following duToit and Wardle [28] we are interested in the mean of the normalized harvested power when the system parameters

**Table 1.** Parameter values used in the simulation.

Parameter	Value	Unit
$m$	$9.12 \times 10^{-3}$	kg
$\bar{k}$	$4.1 \times 10^3$	N m <sup>-1</sup>
$\bar{c}$	0.218	N s m <sup>-1</sup>
$\alpha$	0.8649	—
$R_l$	$3 \times 10^4$	$\Omega$
$\kappa^2$	0.1185	—
$C_p$	$4.3 \times 10^{-8}$	F
$\theta$	$-4.57 \times 10^{-3}$	N V <sup>-1</sup>

are random, that is  $|V|^2/(R_l\omega^4 X_b^2)$ . After some algebra, from equation (15), the normalized power is

$$P = \frac{|V|^2}{R_l\omega^4 X_b^2} = \frac{\bar{k}\alpha\kappa^2}{\bar{\omega}_n^3} \frac{\Omega^2}{\Delta_1(i\Omega, \Psi_\omega, \Psi_\zeta)\Delta_1^*(i\Omega, \Psi_\omega, \Psi_\zeta)}. \quad (16)$$

The average (mean) normalized power can be obtained as

$$\begin{aligned} E[P] &= E\left[\frac{|V|^2}{(R_l\omega^4 X_b^2)}\right] \quad (17) \\ &= \frac{\bar{k}\alpha\kappa^2\Omega^2}{\bar{\omega}_n^3} \int_{-\infty}^{\infty} \int_{-\infty}^{\infty} \frac{f_{\Psi_\omega}(x_1)f_{\Psi_\zeta}(x_2)}{\Delta_1(i\Omega, x_1, x_2)\Delta_1^*(i\Omega, x_1, x_2)} dx_1 dx_2. \quad (18) \end{aligned}$$

The probability density functions (pdf) of  $\Psi_\omega$  and  $\Psi_\zeta$  are denoted by  $f_{\Psi_\omega}(x)$  and  $f_{\Psi_\zeta}(x)$  respectively.

The uncertainty in the coupling coefficient could be addressed in a similar way, and in this case the mean harvested power in equation (18) becomes a triple integral. There is no closed form solution for the double integral case for uncertain natural frequency and damping ratio. Hence, to understand the effect of uncertainty in physical parameters, including the coupling coefficient, we provide numerical evidence from Monte Carlo simulation in section 4.

#### 4. Estimating the mean harvested power by Monte Carlo simulation

In this section we highlight the effect on the harvested power due to uncertainty in the system parameters. To demonstrate the change in harvested power we initially assume that the damping coefficient is known, i.e.  $\Psi_\zeta = 1$ . The uncertainty in the natural frequency is assumed to be a Gaussian random variable with mean one and standard deviation  $\sigma_\omega$ , i.e.  $\Psi_\omega = N(1, \sigma_\omega)$ . Table 1 gives the parameters of the system for the simulations.

Figure 2 shows the mean harvested power ( $E[P]$ ), normalized by  $\omega^4 X_b^2$ , as a function of normalized frequency ( $\Omega$ ) for various values of standard deviation of the natural frequency,  $\sigma_\omega$ . For every value of  $\sigma_\omega$ , a Monte Carlo simulation (MCS) with 5000 samples has been performed. As shown in figure 2, the maximum of the harvested power reduces with the increase in standard deviation of the natural frequency. Figure 3 shows the percentage decrease in the maximum harvested power due to an increase in the standard deviation of the natural frequency graphically. The maximum mean harvested energy with a deterministic natural frequency

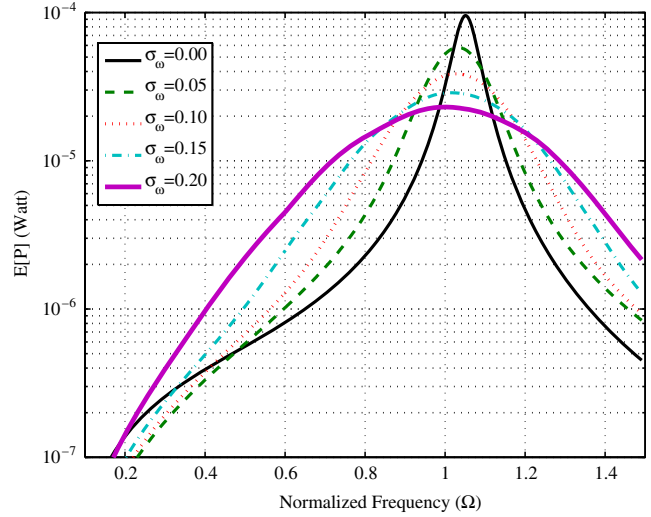


**Figure 2.** The mean power for various values of standard deviation in natural frequency with  $\bar{\omega}_n = 670.5 \text{ rad s}^{-1}$ ,  $\Psi_\zeta = 1$ ,  $\alpha = 0.8649$ ,  $\kappa^2 = 0.1185$ .

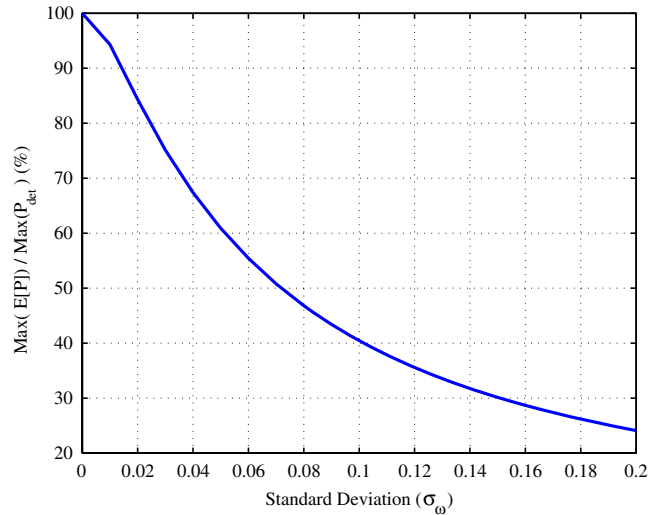
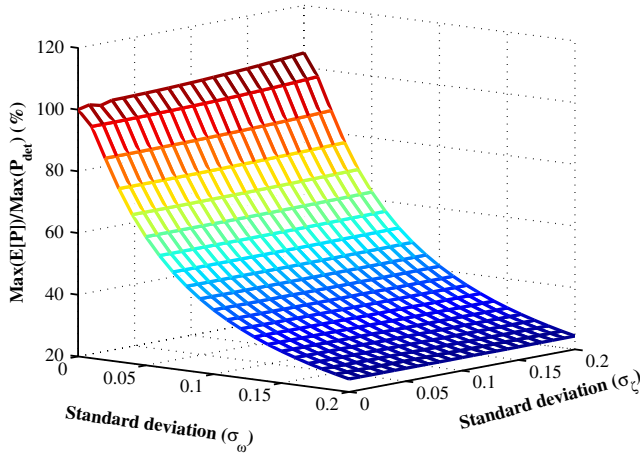


**Figure 3.** The mean harvested power for various values of standard deviation of the natural frequency, normalized by the deterministic power ( $\bar{\omega}_n = 670.5 \text{ rad s}^{-1}$ ,  $\Psi_\zeta = 1$ ,  $\alpha = 0.8649$ ,  $\kappa^2 = 0.1185$ ).

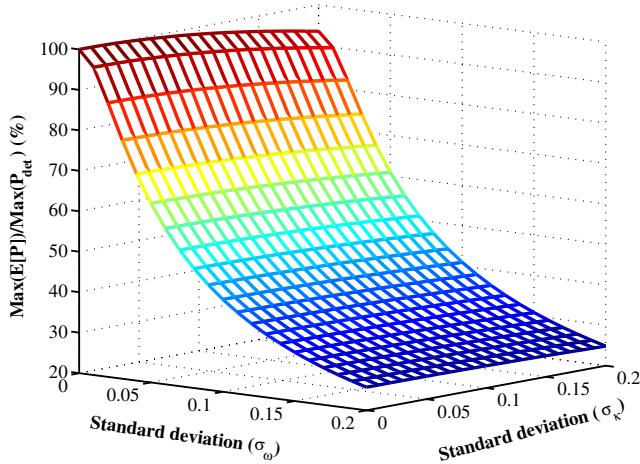
(i.e. with zero standard deviation) is used as a reference. As shown in figure 3 there is an alarming decrease in maximum harvested power of more than 75% for a standard deviation of 20%. This property of the harvested power has received little attention in the literature concerned with energy harvesting. This demonstration motivates us to explore energy harvesting when the system parameters are random.

Figure 4 shows the effect on the harvested power when both natural frequency and damping coefficient are assumed to be independent Gaussian random variables. The change in harvested power with the various values of standard deviation in the damping coefficient ( $\sigma_\zeta$ ) is much lower than the change due to the standard deviation in the natural frequency ( $\sigma_\omega$ ). In deterministic energy harvesters the mechanical damping has a significant effect on the harvested power; however uncertainty





**Figure 4.** The mean harvested power for various values of standard deviation of the natural frequency ( $\sigma_\omega$ ) and damping coefficient ( $\sigma_\zeta$ ), normalized by the deterministic power ( $\bar{\omega}_n = 670.5 \text{ rad s}^{-1}$ ,  $\bar{\zeta} = 0.0178$ ,  $\alpha = 0.8649$ ,  $\kappa^2 = 0.1185$ ).



**Figure 5.** The mean harvested power for various values of standard deviation of the natural frequency ( $\sigma_\omega$ ) and non-dimensional coupling coefficient ( $\sigma_\kappa$ ), normalized by the deterministic power with  $\bar{\omega}_n = 670.5 \text{ rad s}^{-1}$ ,  $\bar{\kappa} = 0.3342$ ,  $\Psi_\zeta = 1$ ,  $\alpha = 0.8649$ .

in the damping leads to realizations where the actual damping ratio is both higher and lower than the mean damping ratio, and as a result the mean harvested power shows little variation as the standard deviation in damping values increases. Indeed the mean harvested power increases slightly as the standard deviation of the damping ratio increases.

Figure 5 shows the decrease in maximum mean power for changes in the standard deviation in natural frequency and non-dimensional coupling coefficient ( $\kappa$ ). The non-dimensional coupling coefficient is also considered to be an independent Gaussian random variable with a maximum standard deviation of 20%. At lower values of uncertainty in natural frequency, the effect of uncertainty in the coupling coefficient has a moderate effect on the maximum mean harvested power. This effect decreases as the uncertainty in natural frequency increases. With the increase in standard deviation in natural frequency the harvested power peak (see figure 2) not only

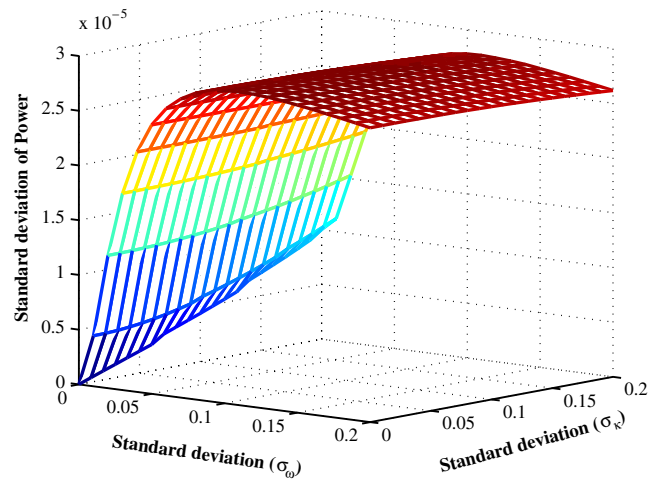


**Figure 6.** The standard deviation of harvested power for various values of standard deviation of the natural frequency ( $\sigma_\omega$ ) and non-dimensional coupling coefficient ( $\sigma_\kappa$ ), normalized by the deterministic power with  $\bar{\omega}_n = 670.5 \text{ rad s}^{-1}$ ,  $\bar{\kappa} = 0.3342$ ,  $\Psi_\zeta = 1$ ,  $\alpha = 0.8649$ .

decreases but also the sharp peak vanishes and the power curve flattens. Therefore, at higher standard deviations in natural frequency, little change in power is observed with uncertainty in the coupling coefficient.

The maximum standard deviation in harvested power for various standard deviations in natural frequency and coupling coefficient is shown in figure 6. The effect of uncertainty in the coupling coefficient is more pronounced at lower values of uncertainty in the natural frequency. Also the uncertainty in power saturates at higher uncertainty levels in natural frequency.

The results given show that the uncertainty in natural frequency has more effect on harvested power than other parametric uncertainties considered (i.e. damping ratio and coupling coefficient). This is expected since variability in the natural frequency, to either lower or higher values, detunes the system away from the excitation frequency and leads to lower harvested power. Thus we now only consider uncertainty in the natural frequency and we explore the effects of the electrical parameters on the harvested power.

### 5. Optimal electrical parameters: semi-analytical approach

One of the main objectives of the design of energy harvesters is to obtain optimal electrical parameters to maximize the harvested energy from harmonic excitation at a fixed frequency. Closed form optimal expressions for the dimensionless electrical time constant,  $\alpha$ , are reported in the literature for the deterministic harvester at zero damping ratio [28] and also with damping [19]. These expressions will be extended to include the effect of a random natural frequency.

The mean harvested power is given by equation (18), which has  $\Delta_1 \times \Delta_1^*$  in the denominator.  $\Delta_1$  is second order in  $x_1$  and first order in  $x_2$ . Thus equation (18) has the fourth power of  $x_1$  and the second power of  $x_2$  in the denominator.

Hence a closed form expression for the mean power cannot be calculated. Section 3 showed that the effect of uncertainty in the damping ratio and electromechanical coupling has less effect on the harvested power than the uncertainty in natural frequency. Hence the damping coefficient is assumed to be deterministic, i.e.  $\Psi_\zeta = x_2 = 1$ . Even after this simplification, an exact closed form expression for the integral in equation (18) cannot be obtained.

### 5.1. Optimal dimensionless time constant, $\alpha$

The goal is to maximize the expected value of power,  $E[P]$ , with respect to the dimensionless time constant,  $\alpha$ . Therefore, the objective function is

$$\min_{\alpha} (-E[P(\alpha)]). \quad (19)$$

The maximum power occurs when  $-\frac{dE[P(\alpha)]}{d\alpha} = 0$ . Thus,

$$\begin{aligned} -\frac{dE[P(\alpha)]}{d\alpha} &= -E\left[\frac{dP(\alpha)}{d\alpha}\right] \\ &= -\frac{\bar{k}\kappa^2\Omega^2}{\bar{\omega}_n^3} E\left[\frac{d}{d\alpha}\left(\frac{\alpha}{\Delta_1\Delta_1^*}\right)\right] \\ &= -\frac{\bar{k}\kappa^2\Omega^2}{\bar{\omega}_n^3} E\left[\frac{\Delta_s - \alpha\frac{d\Delta_s}{d\alpha}}{\Delta_s^2}\right] \end{aligned} \quad (20)$$

where  $\Delta_s = \Delta_1 \times \Delta_1^*$  and is given as

$$\begin{aligned} \Delta_s &= (\Omega^2\alpha^2 + 1)\Psi_\omega^4 + ((4\Omega^4\bar{\zeta}^2 + 2\Omega^2\kappa^2 - 2\Omega^4)\alpha^2 \\ &\quad - 2\Omega^2 + 4\Omega^2\bar{\zeta}^2)\Psi_\omega^2 + 4\Omega^2\bar{\zeta}\Psi_\omega\alpha\kappa^2 \\ &\quad + (\Omega^6 + \Omega^2\kappa^4 - 2\Omega^4\kappa^2)\alpha^2 + \Omega^4. \end{aligned} \quad (21)$$

Setting equation (20) equal to zero, we get

$$\begin{aligned} -\frac{k\kappa^2\Omega^2}{\omega_n^3} E\left[\frac{\Delta_s - \alpha\frac{d\Delta_s}{d\alpha}}{\Delta_s^2}\right] &= 0 \\ E\left[\frac{\Delta_s - \alpha\frac{d\Delta_s}{d\alpha}}{\Delta_s^2}\right] &= 0 \\ E\left[\frac{a_0}{\Delta_s^2}\right] - \alpha^2 E\left[\frac{a_2}{\Delta_s^2}\right] &= 0 \end{aligned} \quad (22)$$

where  $a_0$  and  $a_2$  are given by

$$a_0 = \Psi_\omega^4 + (-2\Omega^2 + 4\Omega^2\bar{\zeta}^2)\Psi_\omega^2 + \Omega^4 \quad (23)$$

$$\begin{aligned} a_2 &= \Psi_\omega^4\Omega^2 + (4\Omega^4\bar{\zeta}^2 + 2\Omega^2\kappa^2 - 2\Omega^4)\Psi_\omega^2 \\ &\quad + \Omega^6 + \Omega^2\kappa^4 - 2\Omega^4\kappa^2. \end{aligned} \quad (24)$$

Equation (22) has to be solved to determine the closed form solution for the optimal value of  $\alpha$ . However, this equation is an implicit equation as the denominator  $\Delta_s^2$  is a function of  $\alpha$  and therefore the solution is not straightforward. Furthermore, equation (22) involves two integrals which are difficult to evaluate. Here we provide an approximate formula for the optimal value of  $\alpha$  by recognizing that if  $\Delta_s^2$  were deterministic then it could be cancelled in (22). Of course  $\Delta_s^2$  will be random, but if this random part is small, relative to the deterministic part, then the random part may be neglected to a first approximation.

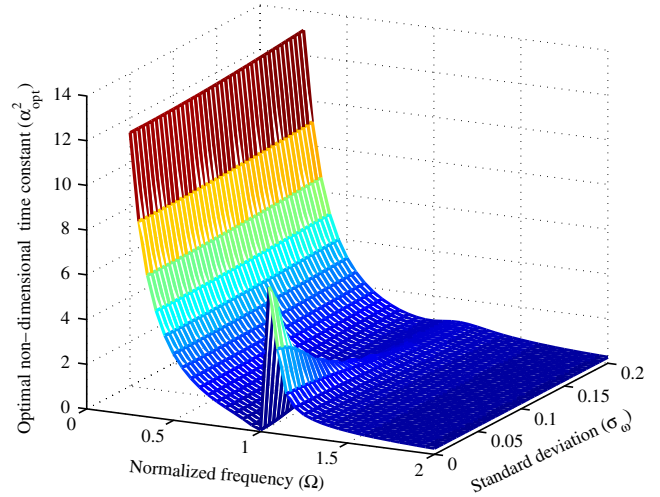


**Figure 7.** The optimal non-dimensional time constant  $\alpha_{\text{opt}}$  for various standard deviations of the natural frequency under harmonic band excitation ( $\bar{\omega}_n = 670.5 \text{ rad s}^{-1}$ ,  $\kappa^2 = 0.1185$ ).

With the above assumptions, we solve equation (22) to give the following expression for the optimal value of  $\alpha$ ,

$$\alpha_{\text{opt}}^2 \approx \frac{E[a_0]}{E[a_2]} = \frac{(c_1 + c_2\sigma_\omega^2 + 3c_3\sigma_\omega^4)}{(c_4 + c_5\sigma_\omega^2 + 3c_6\sigma_\omega^4)} \quad (25)$$

where

$$c_1 = 1 + (4\bar{\zeta}^2 - 2)\Omega^2 + \Omega^4, \quad (26)$$

$$c_2 = 6 + (4\bar{\zeta}^2 - 2)\Omega^2, \quad c_3 = 1,$$

$$c_4 = (1 + 2\kappa^2 + \kappa^4)\Omega^2 + (4\bar{\zeta}^2 - 2 - 2\kappa^2)\Omega^4 + \Omega^6, \quad (27)$$

$$c_5 = (2\kappa^2 + 6)\Omega^2 + (4\bar{\zeta}^2 - 2)\Omega^4, \quad c_6 = \Omega^2, \quad (28)$$

and  $\sigma_\omega$  is the standard deviation in natural frequency.

Note that substituting  $\Psi_\omega = 1$  in equation (22) or  $\sigma_\omega = 0$  in equation (25) gives the deterministic case, and solving for the optimal value of  $\alpha$  gives the expression given in [19]. This deterministic expression is

$$\alpha_{\text{opt}}^2 = \frac{1}{\Omega^2} \frac{(1 - \Omega^2)^2 + (2\bar{\zeta}\Omega)^2}{(1 + \kappa^2 - \Omega^2)^2 + (2\bar{\zeta}\Omega)^2}. \quad (29)$$

Equation (25) therefore can be viewed as the generalization of the deterministic result to the stochastic case.

Figure 7 shows the variation of the optimal value of  $\alpha$  as a function of standard deviation in the natural frequency under harmonic excitation. Figure 7 shows that if the natural frequency is deterministic, a peak for optimal  $\alpha$  occurs at the anti-resonance frequency and this agrees with the results reported by Renno *et al* [19]. This peak gradually decreases as the uncertainty in the natural frequency is increased and almost vanishes at 20% standard deviation.

### 5.2. Optimal dimensionless coupling coefficients, $\kappa$

Proceeding in a similar way to that used to determine optimal non-dimensional time constant (section 5.1), an approximate closed form solution for the optimal non-dimensional coupling

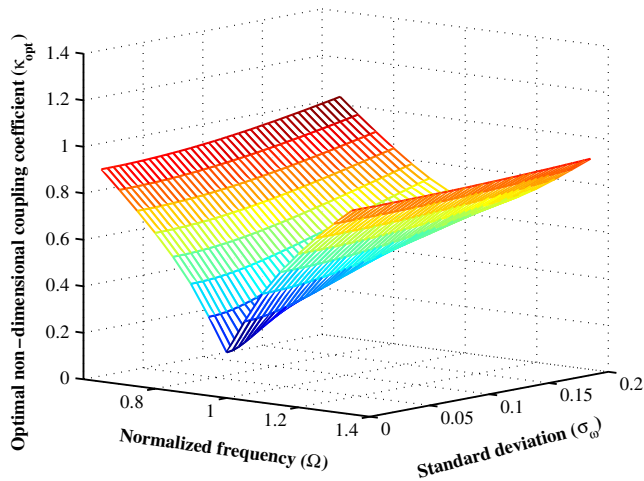


**Figure 8.** The optimal non-dimensional coupling coefficient  $\kappa_{\text{opt}}$  for various standard deviations of the natural frequency under harmonic band excitation ( $\bar{\omega}_n = 670.5 \text{ rad s}^{-1}$ ,  $\alpha = 0.8649$ ).

coefficient,  $\kappa$ , may be obtained. The optimal form of  $\kappa^2$  is given by,

$$\kappa_{\text{opt}}^2 \approx \frac{1}{(\alpha\Omega)} \sqrt{(d_1 + d_2\sigma_\omega^2 + d_3\sigma_\omega^4)} \quad (30)$$

where

$$d_1 = 1 + (4\bar{\zeta}^2 + \alpha^2 - 2)\Omega^2 + (4\bar{\zeta}^2\alpha^2 - 2\alpha^2 + 1)\Omega^4 + \alpha^2\Omega^6 \quad (31)$$

$$d_2 = 6 + (4\bar{\zeta}^2 + 6\alpha^2 - 2)\Omega^2 + (4\bar{\zeta}^2\alpha^2 - 2\alpha^2)\Omega^4 \quad (32)$$

$$d_3 = 3 + 3\alpha^2\Omega^2. \quad (33)$$

Again, if we set  $\sigma_\omega = 0$ , the closed form optimal expression for  $\kappa^2$  as reported in [19] is obtained.

Figure 8 shows the variation of the optimal coupling coefficient  $\kappa$  as a function of the standard deviation of the natural frequency and the non-dimensional frequency  $\Omega$ . Since  $\kappa$  is the coupling coefficient, high values of  $\kappa$  or a zero value are undesirable. In either case the efficiency of the energy transfer between the structural vibration and electrical circuit is low. At zero  $\kappa$ , no energy is transferred to the electrical system. As shown in figure 8 and reported in [19] the coupling coefficient  $\kappa$  attains a minimum value close to the anti-resonance frequency of the system. The value of  $\kappa$  at the anti-resonance increases with the standard deviation. This increment decreases as we move away from the anti-resonance frequency (at both higher and lower frequencies), but the optimal value of  $\kappa$  remains sensitive to variations in the natural frequency at the optimal harvesting frequency.

## 6. Optimal electrical parameters by Monte Carlo simulations

We now analyse the system under parametric uncertainty using Monte Carlo simulation (MCS) [29] and estimate the optimum electrical circuit to maximize the harvested power. The simulation was performed using 5000 sample realizations,

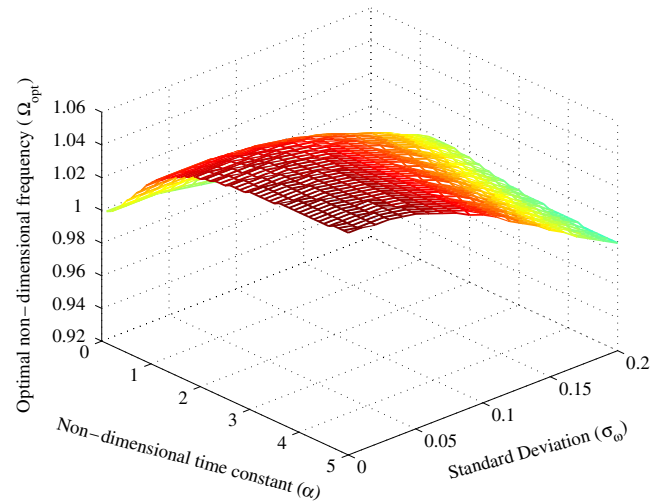


**Figure 9.** The optimal non-dimensional frequency ( $\Omega_{\text{opt}}$ ) obtained using MCS ( $\bar{\omega}_n = 670.5 \text{ rad s}^{-1}$ ,  $\kappa^2 = 0.1185$ ).

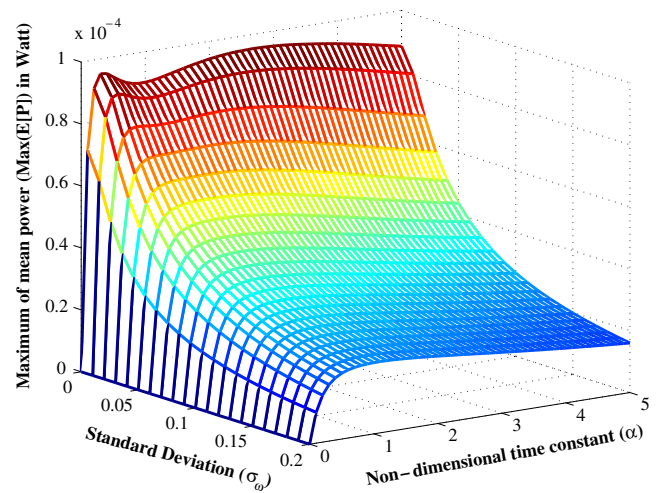


**Figure 10.** The maximum of the mean non-dimensional power ( $\max(E[P])$ ) obtained using MCS ( $\bar{\omega}_n = 670.5 \text{ rad s}^{-1}$ ,  $\kappa^2 = 0.1185$ ).

with the standard deviation of natural frequency between 0 and 20% at an interval of 1%. The non-dimensional time constant  $\alpha$  is varied from 0 to 5 with an interval of 0.1. For the non-dimensional coupling coefficient, the simulation range considered is from 0 to 1 at an interval of 0.05. The optimal values of the parameters lie well within these ranges [19]. For the various simulations, any constant parameters used are given in table 1.

Figure 9 shows the variation in the non-dimensional frequency at which the mean of the harvested power is maximum with the change in the non-dimensional time constant and the standard deviation in natural frequency. The optimal frequency for the maximum harvested power increases with the electrical time constant but decreases with the standard deviation of the natural frequency. Figure 10 shows the non-dimensional harvested power as a function of the electrical time constant and the standard deviation of the



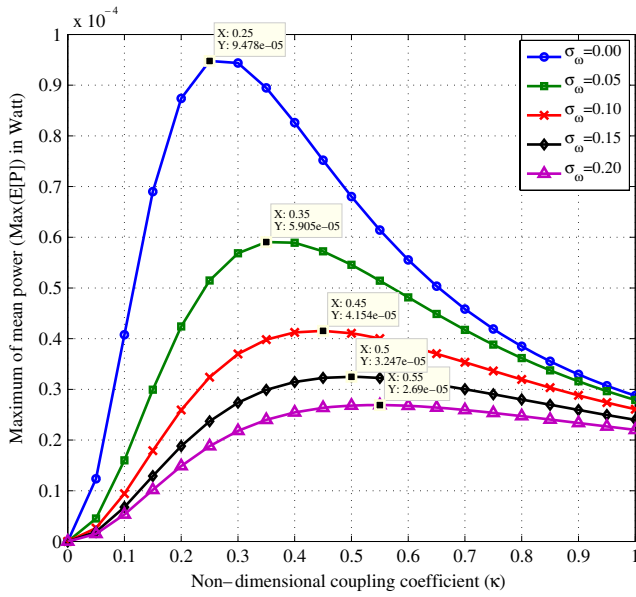


**Figure 11.** The mean non-dimensional power (max(E[P])) obtained using MCS ( $\bar{\omega}_n = 670.5 \text{ rad s}^{-1}$ ,  $\alpha = 0.8649$ ).

natural frequency. The peak of harvested energy decreases with the standard deviation of the natural frequency. One interesting point is that the sharp peak at low values of standard deviation gradually vanishes as the standard deviation increases. The mean harvested power as a function of the non-dimensional coupling coefficient is shown in figure 11 for various values of the standard deviation of the natural frequency. Note the shift in the value of the non-dimensional coupling coefficient at which the mean power is maximum. Figure 11 also shows the points at which the mean harvested power is maximum. The sharp peak at low uncertainty in natural frequency flattens as the uncertainty in natural frequency increases.

It remains to check the accuracy of the approximate analytical expressions for the optimal values of  $\alpha$  and  $\kappa$  by comparison to the MCS results. This is slightly complicated because the analytical approach does not calculate the optimal value of  $\Omega$ . Hence  $\Omega$  is calculated from the MCS results, and then substituted into the equations (25) and (30). Figures 12 and 13 show the comparison with the MCS results and demonstrate that the analytical approach gives the correct trend as the standard deviation varies, and is accurate for low levels of uncertainty.

### 7. Conclusions

Analytical formulations of vibration energy based piezoelectric energy harvesters require many assumptions to obtain a simple model, for example the models generally have a single degree of freedom. These modelling assumptions, together with noise on the measurements, contribute to the uncertainty in parameter identification of the mechanical part of the harvesters. Moreover variability in the parameters during production and material degradation after long use are other sources of parametric variability. This paper has analysed vibration energy based piezoelectric energy harvesters under

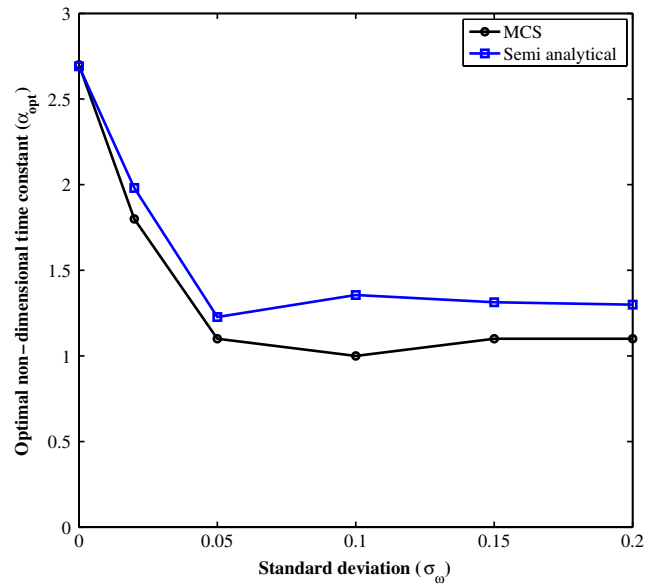


**Figure 12.** Comparison of the optimal non-dimensional time constant  $\alpha_{opt}$  obtained by the analytical approach and MCS.

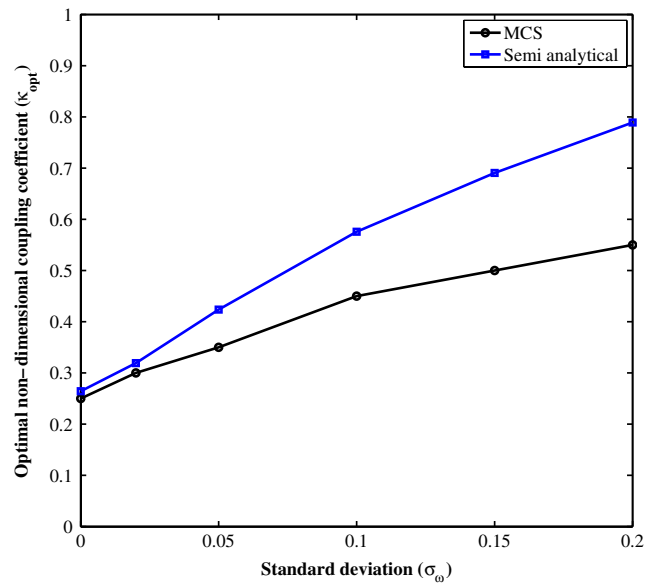


**Figure 13.** Comparison of the optimal non-dimensional coupling coefficient  $\kappa_{opt}$  obtained by the analytical approach and MCS.

parametric uncertainty. Uncertainty in the natural frequency of the system is considered as Gaussian with unit mean and the standard deviation has been varied. Approximate formula for the optimal non-dimensional time constant and optimal non-dimensional coupling coefficient are given and are supported by numerical results using MCS. A graphical insight is given into the effect on the optimal non-dimensional frequency due to the non-dimensional time constant and the standard deviation of the natural frequency. Various insights into the effect of parametric uncertainty on the harvested power are obtained in this paper and are given as follows:

- The mean harvested power decreases abruptly with uncertainty in the natural frequency, as shown by the

approximate analytical results and the Monte Carlo simulation studies;

- The harvested power varies only slightly due to uncertainty in the damping (up to a standard deviation of 20%);
- The sharp peak in the optimal non-dimensional time constant gradually vanishes with increasing standard deviation of the natural frequency;
- The harvested power decreases with increase in uncertainty in coupling coefficient at low uncertainty in natural frequency. As the uncertainty in natural frequency increases the effect of uncertainty in coupling coefficient decreases;
- The value of the non-dimensional coupling coefficient at which the mean harvested power is maximum increases with increasing standard deviation of the natural frequency;
- The optimal value for the non-dimensional frequency decreases with increasing standard deviation of the natural frequency.

## Acknowledgments

SFA gratefully acknowledges the support of Royal Society through the award of a Newton International Fellowship. SA gratefully acknowledges the support of The Leverhulme Trust through the award of the Philip Leverhulme Prize.

## References

- [1] Anton S R and Sodano H A 2007 A review of power harvesting using piezoelectric materials (2003–2006) *Smart Mater. Struct.* **16** R1–21
- [2] Beeby S P, Tudor M J and White N M 2006 Energy harvesting vibration sources for microsystems applications *Meas. Sci. Technol.* **17** R175–95
- [3] Lefeuvre E, Badel A, Benayad A, Lebrun L, Richard C and Guyomar D 2005 A comparison between several approaches of piezoelectric energy harvesting *J. Physique IV* **128** 177–86
- [4] Lefeuvre E, Badel A, Richard C, Petit L and Guyomar D 2006 A comparison between several vibration-powered piezoelectric generators for standalone systems *Sensors Actuators A* **126** 405–16
- [5] Priya S 2007 Advances in energy harvesting using low profile piezoelectric transducers *J. Electroceram.* **19** 167–84
- [6] Sodano H, Inman D and Park G 2004 A review of power harvesting from vibration using piezoelectric materials *Shock Vib. Dig.* **36** 197–205
- [7] Sodano H, Inman D and Park G 2005 Generation and storage of electricity from power harvesting devices *J. Intell. Mater. Syst. Struct.* **16** 67–75
- [8] Tanner T and Inman D J 2002 Combined shock and vibration isolation through the optimal control of hybrid ‘smart’ mount *Proc. 73rd Shock and Vibration Symp. (Newport Beach, RI)*
- [9] Adhikari S, Friswell M I and Inman D J 2009 Piezoelectric energy harvesting from broadband random vibrations *Smart Mater. Struct.* **18** 115005
- [10] Litak G, Friswell M I and Adhikari S 2010 Magnetopiezoelectric energy harvesting driven by random excitations *Appl. Phys. Lett.* **96** 214103
- [11] Soliman M S M, Abdel-Rahman E M, El-Saadany E F and Mansour R R 2008 A wideband vibration-based energy harvester *J. Micromech. Microeng.* **18** 115021
- [12] Liu F, Phipps A, Horowitz S, Ngo K, Cattafesta L, Nishida T and Sheplak M 2008 Acoustic energy harvesting using an electromechanical Helmholtz resonator *J. Acoust. Soc. Am.* **123** 1983–90
- [13] Shu Y C and Lien I C 2006 Efficiency of energy conversion for a piezoelectric power harvesting system *J. Micromech. Microeng.* **16** 2429–38
- [14] Shu Y C and Lien I C 2006 Analysis of power output for piezoelectric energy harvesting systems *Smart Mater. Struct.* **15** 1499–512
- [15] Shu Y C, Lien I C and Wu W J 2007 An improved analysis of the SSHI interface in piezoelectric energy harvesting *Smart Mater. Struct.* **16** 2253–64
- [16] Ng T and Liao W 2005 Sensitivity analysis and energy harvesting for a self-powered piezoelectric sensor *J. Intell. Mater. Syst. Struct.* **16** 785–97
- [17] duToit N, Wardle B and Kim S 2005 Design considerations for MEMS-scale piezoelectric mechanical vibration energy harvesters *Integr. Ferroelectr.* **71** 121–60
- [18] Roundy S 2005 On the effectiveness of vibration-based energy harvesting *J. Intell. Mater. Syst. Struct.* **16** 809–23
- [19] Renno J M, Daqaq M F and Inman D J 2009 On the optimal energy harvesting from a vibration source *J. Sound Vib.* **320** 386–405
- [20] Kompella M S and Bernhard B J 1993 Measurement of the statistical variations of structural-acoustics characteristics of automotive vehicles *SAE Noise and Vibration Conf.* (Warrendale: Society of Automotive Engineers)
- [21] Fahy F 2000 *Foundations of Engineering Acoustics* (London: Academic)
- [22] Adhikari S, Friswell M I, Lonkar K and Sarkar A 2009 Experimental case studies for uncertainty quantification in structural dynamics *Probab. Eng. Mech.* **24** 473–92
- [23] Adhikari S and Friswell M I 2007 Random matrix eigenvalue problems in structural dynamics *Int. J. Numer. Methods Eng.* **69** 562–91
- [24] Erturk A and Inman D J 2009 An experimentally validated bimorph cantilever model for piezoelectric energy harvesting from base excitations *Smart Mater. Struct.* **18** 025009
- [25] Erturk A and Inman D J 2008 A distributed parameter electromechanical model for cantilevered piezoelectric energy harvesters *Trans. ASME, J. Vib. Acoust.* **130** 041002
- [26] Erturk A and Inman D J 2008 On mechanical modeling of cantilevered piezoelectric vibration energy harvesters *J. Intell. Mater. Syst. Struct.* **19** 1311–25
- [27] Erturk A and Inman D J 2008 Issues in mathematical modeling of piezoelectric energy harvesters *Smart Mater. Struct.* **17** 065016
- [28] duToit N E and Wardle B L 2007 Experimental verification of models for microfabricated piezoelectric vibration energy harvesters *AIAA J.* **45** 1126–37
- [29] Rubinstein R Y and Kroese D 2008 *Simulation and the Monte Carlo Method* (Hoboken, NJ: Wiley Interscience)